during the occlusion. Immediately after occlusion, the O_2 content decreased rapidly. The HbV_8 group showed a slower rate of reduction compared with the HbV_{29} group and the group before HbV infusion. To demonstrate the contribution of HbVs clearly, only the O_2 content of HbVs is shown in Fig. 5*B*. HbV_8 showed a very slow rate of O_2 release. After 30 s of occlusion, the arteriolar P_{O_2} decreased to 5.2 ± 0.7 mmHg. However, $Sa_{O_2}(HbV_8)$ was 26.1 ± 7.3% and did not reach steady state but continued O_2 release. HbV_{29} showed almost no change after 15 s, and $Sa_{O_2}(HbV_{29})$ was 7.4 ± 1.0% after 30 s. Figure 5*C* shows the rate of O_2 loss from HbVs obtained by the differentiation of the graphs in Fig. 5B. HbV_{29} showed the fastest O_2 loss with the maximum of 0.18 ml O_2/dl blood sec after only 2 s of occlusion and did not supply O_2 after 17 s. On the other hand, HbV_8 showed a moderate O_2 loss and showed the maximum of 0.08 ml O_2/dl blood after 10 s of occlusion and continued to release O_2 until 30 s.

Figure 6 shows the fraction of O_2 in blood originating from HbVs. Before occlusion of the arterioles, the fractions of HbV_8 and HbV_{29} are very small and similar because of the small dosage compared with the originally present RBCs. However, after occlusion, the fraction of O_2 from HbV_8 increased significantly and was about 0.55 after 10 s. This indicated that HbV_8, and not RBCs, was the main source of the O_2 carrier when P_{O_2} attained very low values.

DISCUSSION

The principal finding of this study is that HbV_8 (P_{50} = 8 mmHg) with a high O_2 affinity (low P_{50}) releases O_2 at a slower rate than does HbV_{29} in occluded arterioles of the hamster dorsal skinfold model. Furthermore, we found that HbV_8, and not HbV_{29}, is the main O_2 source in ischemic conditions.

The immediate occlusion of blood flow in the arterioles caused a rapid reduction of O_2 content. Similar phenomena have been observed by Richmond et al. (23) in rat spinotrapezius muscle tissue. There is substantial evidence that the arteriolar wall is a significant O_2 sink, consuming O_2 at a rate that is much greater than most tissues (9, 35, 42), which explains in part the significant and rapid drop of P_{O_2} found in our study. In our experiments, only one arteriole was occluded at a time in the intact subcutaneous tissue, and arteriolar P_{O_2} decreased to about 5 mmHg, which was higher than the critical P_{O_2} (2.9 ± 0.5 mmHg) in the rat spinotrapezius muscle tissue (23). Although the O_2 supply was significantly reduced, diffusion of O_2 from the other surrounding arterioles, venules, and capillaries near the occlusion should contribute to maintaining tissue P_{O_2} at a higher value than in the study of Richmond et al. (23), where the supply of blood to the tissue was stopped altogether. $Sa_{O_2}(HbV_8)$ at 5 mmHg is estimated to be about 26% according to the OECs (Fig. 1), which is higher than that for HbV_{29} (6%) and RBCs (2%); thus HbV_8 remains a source of O_2 for a longer period in a prolonged occlusion, because the fraction of O_2 from HbV_8 was 0.5 or higher, overwhelming the contribution from RBCs, as shown in Fig. 6.

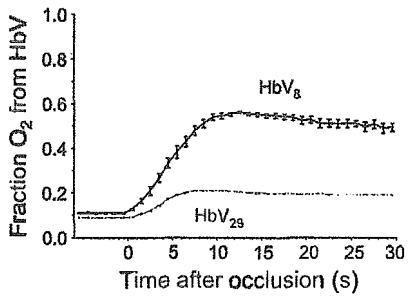

Fig. 6. Time course of the fraction of O_2 content from HbVs in whole blood. The extended time of occlusion induced hypoxic conditions and the fraction of O_2 content from HbV_8 increased significantly compared with HbV_{29}.

A limitation of our experimental method is that Sa_{O_2} is estimated under the assumption that conditions in the target arteriole are identical to that of the OEC measurement; however, the O_2 affinity of Hb changes as a function of temperature, pH, electrolyte concentration, and CO_2 content. Local ischemic conditions caused by the occlusion could affect pH and increase CO_2 tension, resulting in a slight decrease in the O_2 affinity (increased P_{50}); however, it is unlikely that this would introduce a significant error in the measurement of O_2 release considering the short duration of the occlusion (30 s).

We have previously demonstrated using an artificial narrow polymer tube (inner diameter: 28 μm) surrounded by a sodium dithionate solution to consume O_2 that a Hb solution under continuous flow conditions (1 mm/s) facilitates O_2 release when mixed with RBCs. Conversely, HbV did not show this phenomenon (31). This difference is due to the small size of O_2-bound acellular Hb molecules, which diffuse and therefore contribute to the facilitated O_2 transport (21, 31), whereas HbVs (diameter, about 250 nm) are too large to show sufficient diffusion for the facilitated O_2 transport. In these conditions, O_2 affinity (P_{50}) becomes the determining factor for the rate of O_2 release and transport to the vessels wall. Thus, in our present results, the presence of HbVs did not facilitate the reduction of P_{O_2} or O_2 content but retarded the reduction of P_{O_2} and O_2 content.

Our experimental model is designed to characterize the O_2 release behavior of blood from an occluded microvessel and does not directly related to clinical ischemic conditions because the occlusion of the small arteriole for 30 s does not induce tissue ischemia other than the transient event in the proximity of the microvessel. However, our data suggest that HbV_8 could be a significant source of O_2 in an ischemic condition with significantly lowered tissue P_{O_2}. Because of the small dosage of HbV_8 (7 ml/kg), the O_2 content in the blood after occlusion (5 ml O_2/dl blood at 5 s) is significantly smaller than the baseline value (20 ml O_2/dl blood at 0 s). To enhance the contribution of HbVs, a larger dosage and sustained blood flow would be required. Contaldo et al. (7) recently demonstrated that inducing hemodilution using up to 50% blood exchange with HbV (P_{50} = 15 mmHg) suspended in dextran effectively oxygenated ischemic collaterized tissue in skin flaps. This phenomenon could be explained by low P_{50} HbVs retaining O_2 in the upstream vessels and delivering it to the ischemic tissue via collateral arterioles, even when these may have significantly slower blood flow. It has been proposed that small-sized HBOCs oxygenate ischemic tissue by being able to pass through constricted or partially occluded vessels that do not allow the passage of RBCs; however, the results from Contaldo et al. (17) as well as those from our experimental model do not serve to support this concept, because arterioles were completely ligated or occluded. It should be noted, however, that an advantage of small HBOCs, including HbVs,

is that they are homogeneously dispersed in the plasma phase and therefore can deliver O_2 more homogeneously to the periphery than RBCs because microvascular hematocrit is heterogeneous particularly in pathological states. In such conditions, HbVs with a higher O_2 affinity should show a slower O_2 unloading that would be effective for oxygenating ischemic tissues.

In conclusion, HbVs provide the unique feature of allowing for the regulation of P_{50} by modulating the amount of coencapsulated PLP (33, 45). Recent studies showed the effectiveness of HBOCs with a lower P_{50} (higher O_2 affinity) as a means of implementing O_2 delivery targeted to ischemic tissue (2, 3, 41, 43). Thus this experimental method provides data useful for the design and optimization of O_2 carriers and suggests the possible utilization of HbVs for therapeutic approaches aimed at remedying ischemic conditions.

ACKNOWLEDGMENTS

The authors greatly acknowledge A. Barra and C. Walser (University of California-San Diego) for help with the animal preparations, Dr. S. Takeoka and Dr. K. Sou (Waseda University) for the preparation of the HbVs, and Dr. D. Erni (Inselspital University Hospital, Bern, Switzerland) for meaningful discussions.

GRANTS

This study was supported in part by Health Sciences Research grants (Regulatory Science, Artificial Blood Project); the Ministry of Health, Labour and Welfare, Japan (H16-IYAKU-069, 071); Japan Society for the Promotion of Science Grant-In-Aid for Scientific Research B16300162; and National Heart, Lung, and Blood Institute Bioengineering Partnership Grant R24 HL-64395 and Grants R01 HL-40696 and R01 HL-62354. H. Sakai was an overseas research fellow of the Society of Japanese Pharmacopoeia.

REFERENCES

1. **Awasthi VD, Garcia D, Klipper R, Goins BA, and Phillips WT.** Neutral and anionic liposome-encapsulated hemoglobin: effect of postinserted poly(ethylene glycol)-distearoylphosphatidylethanolamine on distribution and circulation kinetics. *J Pharmacol Exp Ther* 309: 241–248, 2004.
2. **Baines AD, Adamson G, Wojciechowski P, Pliura D, Ho P, and Kluger R.** Effect of modifying O_2 diffusivity and delivery on glomerular and tubular function in hypoxic perfused kidney. *Am J Physiol Renal Physiol* 274: F744–F752, 1998.
3. **Baines AD and Ho P.** O_2 affinity of cross-linked hemoglobins modifies O_2 metabolism in proximal tubules. *J Appl Physiol* 95: 563–570, 2003.
4. **Buehler PW and Alayash AI.** Toxicities of hemoglobin solutions: in search of in-vitro and in-vivo model systems. *Transfusion* 44: 1516–1530, 2004.
5. **Chang TMS.** *Blood Substitutes: Principles, Methods, Products, and Clinical Trials.* Basel: Karger, 1997.
6. **Cabrales P, Sakai H, Tsai AG, Tsuchida E, and Intaglietta M.** Oxygen transport by low and normal P_{50} hemoglobin vesicles in extreme hemodilution. *Am J Physiol Heart Circ Physiol* 288: H1885–H1892, 2005. First published November 24, 2004; doi:10.1152/ajpheart.01004.2004.
7. **Contaldo C, Schramm S, Wettstein R, Sakai H, Takeoka S, Tsuchida E, Leunig M, Banic A, and Erni D.** Improved oxygenation in ischemic hamster flap tissue is correlated with increasing hemodilution with Hb vesicles and their O_2 affinity. *Am J Physiol Heart Circ Physiol* 285: H1140–H1147, 2003.
8. **Djordjevich L, Mayoral J, Miller IF, and Ivankovich AD.** Cardiorespiratory effects of exchange transfusions with synthetic erythrocytes in rats. *Crit Care Med* 15: 318–323, 1987.
9. **Duling BR and Berne RM.** Longitudinal gradients in periarteriolar oxygen tension. A possible mechanism for the participation of oxygen in the local regulation of blood flow. *Circ Res* 27: 669–678, 1970.
10. **Endrich B, Asaishi K, Gotz A, and Messmer K.** Technical report: a new chamber technique for microvascular studies inunanesthetized hamsters. *Res Exp Med (Berl)* 177: 125–134, 1980.
11. **Erni D, Wettstein R, Schramm S, Sakai H, Takeoka S, Tsuchida E, Leunig M, and Banic A.** Normovolemic hemodilution with hemoglobin-vesicle solution attenuates hypoxia in ischemic hamster flap tissue. *Am J Physiol Heart Circ Physiol* 284: H1702–H1709, 2003.
12. **Goda N, Suzuki K, Naito S, Takeoka S, Tsuchida E, Ishimura Y, Tamatani T, and Suematsu M.** Distribution of heme oxygenase isoform in rat liver: topographic basis for carbon monoxide-mediated micorvascular relaxation. *J Clin Invest* 101: 604–612, 1998.
13. **Intaglietta M, Johnson PC, and Winslow RM.** Microvascular and tissue oxygen distribution. *Cardiovasc Res* 32: 632–643, 1996.
14. **Intaglietta M, Silverman NR, and Tompkins WR.** Capillary flow velocity measurements in vivo and in situ by television methods. *Microvasc Res* 10: 165–179, 1975.
15. **Intaglietta M and Tompkins WR.** Microvascular measurements by video image shearing and splitting. *Microvasc Res* 5: 309–312, 1973.
16. **Izumi Y, Sakai H, Hamada K, Takeoka S, Yamahata Y, Kato R, Nishide H, Tsuchida E, and Kobayashi K.** Physiologic responses to exchange transfusion with hemoglobin vesicles as an artificial oxygen carrier in anesthetized rats: changes in mean arterial pressure and renal cortical tissue oxygen tension. *Crit Care Med* 24: 1869–1873, 1996.
17. **Kerger H, Torres Filho IP, Rivas M, Winslow RM, and Intaglietta M.** Systemic and subcutaneous microvascular oxygen tension in conscious Syrian golden hamsters. *Am J Physiol Heart Circ Physiol* 268: H802–H810, 1995.
18. **Kyokane Norimuzu S T, Taniai H, Yamaguchi T, Takeoka S, Tsuchida E, Naito M, Nimura Y, Ishimura Y, and Suematsu M.** Carbon monoxide from heme catabolism protects against hepatobiliary dysfunction in endotoxin-treated rat liver. *Gastroenterology* 120: 1227–1240, 2001.
19. **Linberg R, Conover CD, Shum KL, and Shorr RGL.** Increased tissue oxygenation and enhanced radiation sensitivity of solid tumors in rodents following polyethylene glycol conjugated bovine hemoglobin administration. In Vivo 12: 167–174, 1998.
20. **Lipowsky HH and Zweifach B.** Application of the "two slit" photometric technique to the measurement of microvascular volumetric flow rates. *Microvasc Res* 15: 93–101, 1978.
21. **McCarthy MR, Vandegeriff KD, and Winslow RM.** The role of facilitated diffusion in oxygen transport by cell-free hemoglobins: implications for the design of hemoglobin-based oxygen carriers. *Biophys Chem* 92: 103–117, 2001.
22. **Papenfuss HD, Gross JF, Intaglietta M, and Treese FA.** A transparent access chamber for the rat dorsal skin fold. *Microvasc Res* 18: 311–318, 1979.
23. **Richmond KN, Shonat RD, Lynch RM, and Johnson PC.** Critical P_{O_2} of skeletal muscle in vivo. *Am J Physiol Heart Circ Physiol* 277: H1831–H1840, 1999.
24. **Rudolph AS, Klipper RW, Goins B, and Phillips WT.** In vivo biodistribution of a radiolabelled blood substitute: ^{99m}Tc-labeled liposome-encapsulated hemoglobin in an anesthetized rabbit. *Proc Natl Acad Sci USA* 88: 10976–10980, 1991.
25. **Sakai H, Hara H, Tsai AG, Tsuchida E, Johnson PC, and Intaglietta M.** Changes in resistance vessels during hemorrhagic shock and resuscitation in conscious hamster model. *Am J Physiol Heart Circ Physiol* 276: H563–H571, 1999.
26. **Sakai H, Hara H, Yuasa M, Tsai AG, Takeoka S, Tsuchida E, and Intaglietta M.** Molecular dimensions of Hb-based O_2 carriers determine constriction of resistance arteries and hypertension in conscious hamster model. *Am J Physiol Heart Circ Physiol* 279: H908–H915, 2000.
27. **Sakai H, Hisamoto S, Fukutomi I, Sou K, Takeoka S, and Tsuchida E.** Detection of lipopolysaccharide in hemoglobin-vesicles by *Limulus amebocyte* lysate test with kinetic-turbidimetric gell clotting analysis and pretreatment with a surfactant. *J Pharm Sci* 93: 310–321, 2004.
28. **Sakai H, Horinouchi H, Tomiyama K, Ikeda E, Takeoka S, Kobayashi K, and Tsuchida E.** Hemoglobin-vesicles as oxygen carriers: influence on phagocytic activity and histopathological changes in reticuloendothelial systems. *Am J Pathol* 159: 1079–1088, 2001.
29. **Sakai H, Masada Y, Horinouchi H, Ikeda E, Sou K, Takeoka S, Suematsu M, Kobayashi K, and Tsuchida E.** Physiologic capacity of reticuloendothelial system for degradation of hemoglobin-vesicles (artificial oxygen carriers) after massive intravenous doses by daily repeated infusion for 14 days. *J Pharmacol Exp Ther* 311: 874–884, 2004.
30. **Sakai H, Masada Y, Horinouchi H, Yamamoto M, Ikeda E, Takeoka S, Kobayashi K, and Tsuchida E.** Hemoglobin-vesicles suspended in recombinant human serum albumin for resuscitation from hemorrhagic shock in anesthetized rats. *Crit Care Med* 32: 539–545, 2004.

31. **Sakai H, Suzuki Y, Kinoshita M, Takeoka S, Maeda N, and Tsuchida E.** O_2-release from Hb-vesicles evaluated using an artificial narrow O_2-permeable tube: comparison with RBC and acellular Hb. *Am J Physiol Heart Circ Physiol* 285: H2543–H2551, 2003.
32. **Sakai H, Takeoka S, Yokohama H, Seino Y, Nishide H, and Tsuchida E.** Purification of concentrated Hb using organic solvent and heat treatment. *Protein Expr Purif* 4: 563–569, 1993.
33. **Sakai H, Tsai AG, Rohlfs RJ, Hara H, Takeoka S, Tsuchida E, and Intaglietta M.** Microvascular responses to hemodilution with Hb-vesicles as red blood cell substitutes: influences of O_2 affinity. *Am J Physiol Heart Circ Physiol* 276: H553–H562, 1999.
34. **Sakai H, Yuasa M, Onuma H, Takeoka S, and Tsuchida E.** Synthesis and physicochemical characterization of a series of hemoglobin-based oxygen carriers: objective comparison between cellular and acellular types. *Bioconjug Chem* 11: 56–64, 2000.
35. **Shibata M, Ichioka S, Ando J, and Kamiya A.** Microvascular and interstitial P_{O_2} measurements in rat skeletal muscle by phosphorescence quenching. *J Appl Physiol* 91: 321–327, 2001.
36. **Shirasawa T, Izumizaki M, Suzuki YI, Ishihara A, Shimizu T, Tamaki M, Huang F, Koizumi KI, Iwase M, Sakai H, Tsuchida E, Ueshima U, Inoue H, Koseki H, Senda H, Kuriyama T, and Homma I.** Oxygen affinity of hemoglobin regulates O_2 consumption, metabolism, and physical activity. *J Biol Chem* 278: 5035–5043, 2003.
37. **Sou K, Naito Y, Endo T, Takeoka S, and Tsuchida E.** Effective encapsulation of proteins into size-controlled phospholipid vesicles using freeze-thawing and extrusion. *Biotechnol Progr* 19: 1547–1552, 2003.
38. **Takeoka S, Teramura Y, Atoji T, and Tsuchida E.** Effect of Hb-encapsulation with vesicles on H_2O_2 reaction and lipid peroxidation. *Bioconjug Chem* 13: 1302–1308, 2002.
39. **Tomson FN and Wardrop KJ.** Clinical chemistry and hematology. In: *Laboratory Hamsters*, edited by van Hoosier GL Jr and McPherson CW. Orlando, FL: Academic, 1987, chapt. 3, p. 43–59.
40. **Torres Filho IP and Intaglietta M.** Microvascular P_{O_2} measurements by phosphorescence decay method. *Am J Physiol Heart Circ Physiol* 265: H1434–H1438, 1993.
41. **Tsai AG, Kerger H, and Intaglietta M.** Microcirculatory consequences of blood substitutution with αα-hemoglobin. In: *Blood Substitutes: Physiological Basis of Efficacy*, edited by Winslow RM, Vandegriff K, and Intaglietta M. Boston, MA: Birkhauser, 1995, p. 155–174.
42. **Tsai AG, Friesenecker B, Mazzoni MC, Kerger H, Buerk DG, Johnson PC, and Intaglietta M.** Microvascular and tissue oxygen gradients in the rat mesentery. *Proc Natl Acad Sci USA* 95: 6590–6595, 1998.
43. **Tsai AG, Vandegriff KD, Intaglietta M, and Winslow RM.** Targeted O_2 delivery by low-P_{50} hemoglobin: a new basis for O_2 therapeutics. *Am J Physiol Heart Circ Physiol* 285: H1411–H1419, 2003.
44. **Vanderkooi JM, Maniara G, Green TJ, and Wilson DF.** An optical method for measurement of dioxygen concentration based on quenching of phosphorescence. *J Biol Chem* 262: 5476–5482, 1987.
45. **Wang L, Morizawa K, Tokuyama S, Satoh T, and Tsuchida E.** Modulation of oxygen-carrying capacity of artificial red cells (ARC). *Polymer Adv Technol* 4: 8–11, 1992.

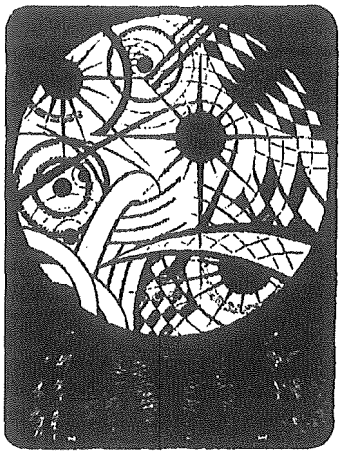

Am J Physiol Heart Circ Physiol 289: H2624–H2631, 2005.
First published August 5, 2005; doi:10.1152/ajpheart.00308.2005.

Is hemoglobin in hemoglobin vesicles infused for isovolemic hemodilution necessary to improve oxygenation in critically ischemic hamster skin?

Jan A. Plock,[1] Claudio Contaldo,[1] Hiromi Sakai,[2] Eishun Tsuchida,[2] Michael Leunig,[1] Andrej Banic,[1] Michael D. Menger,[3] and Dominique Erni[1]

[1]*Department of Orthopedic, Plastic and Hand Surgery, Inselspital University Hospital, Berne, Switzerland;*
[2]*Advanced Research Institute for Science and Engineering, Waseda University, Tokyo, Japan; and*
[3]*Institute for Clinical and Experimental Surgery, University of Saarland, Homburg/Saar, Germany*

Submitted 30 March 2005; accepted in final form 31 July 2005

Plock, Jan A., Claudio Contaldo, Hiromi Sakai, Eishun Tsuchida, Michael Leunig, Andrej Banic, Michael D. Menger, and Dominique Erni. Is hemoglobin in hemoglobin vesicles infused for isovolemic hemodilution necessary to improve oxygenation in critically ischemic hamster skin? *Am J Physiol Heart Circ Physiol* 289: H2624–H2631, 2005. First published August 5, 2005; doi:10.1152/ajpheart.00308.2005.—The aim of this study was to test the influence of hemoglobin, encapsulated in phospholipid vesicles as an oxygen carrier, given in the course of isovolemic hemodilution to improve oxygenation in critically ischemic hamster flap tissue. Capillary hemodynamics and macromolecular leakage were investigated with intravital microscopy and analyzed off-line with the CapImage software. Partial tissue oxygen tension was measured with fluorescence quenching electrodes. The occurrence of apoptosis was assessed with the terminal deoxynucleotidyl transferase-mediated dUTP nick-end labeling assay. Vesicles with (HbV) or without (V) encapsulated Hb were suspended in 6% hydroxyethyl starch (HES) used for the 33% blood exchange. In the ischemic tissue, hemodilution led to an increase in functional capillary density by 31% for HES ($P < 0.01$ vs. other groups), 66% for V-HES, and 62% for HbV-HES (all $P < 0.01$ vs. control). Capillary diameters behaved inversely proportional to capillary microhemodynamics. The 20% increase in macromolecular leakage found over time in control animals was completely abolished in the vesicles groups ($P < 0.01$) but not with HES. Oxygen tension was improved from 10.7 to 16.0 mmHg after HbV-HES ($P < 0.01$ vs. baseline and other groups). Compared with the other groups, apoptosis was significantly reduced after HbV-HES ($P < 0.01$). We conclude that the encapsulation of Hb was essential to attenuate hypoxia and subsequent cell death in the critically ischemic tissue. However, the effect was partly attributed to the rheological changes exerted by the vesicles.

blood substitutes; capillary hemodynamics; hypoxia; capillary leakage; apoptosis

CRITICAL ISCHEMIA is characterized by a reduction of nutrient blood flow, thus causing hypoxia that may eventually lead to apoptosis and cell death. One of the most frequent etiologies of critical ischemia is the acute peripheral arterial obstruction. Oxygenation and survival of ischemic myocardial (13, 24), cerebral (23, 32), and peripheral (6) tissues could successfully be improved after the infusion of solutions containing artificial oxygen carriers, such as perfluorocarbons and chemically modified Hbs.

In recent studies (8, 12), we were able to demonstrate that hypoxia in ischemic hamster flap tissue was attenuated by isovolemic hemodilution with colloid solutions supplemented with phospholipid vesicles containing isolated, purified human Hb. The effect was ascribed to the combination of an improvement of the impaired microcirculation and the presence of the Hb vesicles (HbVs) (12), and it correlated with the degree of blood exchange (8). However, it was not possible to outline the extent to which either the rheological changes or the presence of Hb contributed to this benefit. In other words, it could not be excluded that similar success could have been achieved with the use of phospholipid vesicles void of oxygen carriers, which in turn would have a significant impact on their clinical application, because the manufacturing of the vesicles could be simplified and possible adverse effects related to the encapsulated Hb could be avoided. Furthermore, it may be postulated that the presence of cell-free Hbs may lead to arteriolar vasoconstriction with (4, 26) or without (14) scavenging of nitric oxide, which may further deteriorate microvascular perfusion and oxygen delivery in the ischemic tissue.

In this context, the viscosity of the diluent appears to play a pivotal role. Because of the large size of the vesicles, the viscosity of HbV solutions is manyfold higher than that of hamster plasma (12, 26). Raising the viscosity in the plasma phase of the circulating blood led to shear stress-induced, nitric oxide-mediated arteriolar vasodilation (2, 9), which was made responsible for increasing microcirculatory blood flow (2), microvascular pressure (3), and functional capillary density (FCD) (2, 3) in healthy tissue in hamsters. Furthermore, according to the Stokes-Einstein equation, the diffusivity of oxygen through the plasma is inversely proportional to its viscosity, an effect that may contribute to the distribution of oxygen release in favor of hypoxic tissues, in which oxygen diffusion is ensured by the high gradient of partial oxygen tension.

The hypothesis to be tested in this study was whether the presence of Hb in the HbV is needed to obtain the previously reported benefit of isovolemic hemodilution with HbV on the oxygenation of the ischemic hamster flap tissue (8, 12) or whether similar effects could be obtained with a suspension of vesicles void of Hb due to their viscosity-related effect on arteriolar and capillary hemodynamics and on tissue oxygenation.

MATERIALS AND METHODS

Experiments were performed according to the National Institutes of Health guidelines for the care and use of laboratory animals and with

Address for reprint requests and other correspondence: D. Erni, Division of Plastic and Reconstructive Surgery, Inselspital Univ. Hospital, CH-3010 Berne, Switzerland (e-mail: dominique.erni@insel.ch).

The costs of publication of this article were defrayed in part by the payment of page charges. The article must therefore be hereby marked "*advertisement*" in accordance with 18 U.S.C. Section 1734 solely to indicate this fact.

the approval of the local Animal Ethics Committee. Forty-eight male Syrian golden hamsters weighing 65–85 g were used in this study. The animals were randomly assigned to the control group or to one of three groups subjected to normovolemic hemodilution with 6% hydroxyethyl starch 200–0.5 (HES; Fresenius, Stans, Switzerland) or vesicles with or without encapsulated Hb suspended in hydroxyethyl starch (HbV-HES and V-HES, respectively).

Animal and flap preparation. A hamster skin flap model was used as previously described in detail (7, 8, 10–12). Anesthesia was induced by pentobarbital sodium (Nembutal) injected intraperitoneally (100 mg/kg body wt; Abbott Laboratories, Chicago, IL). The carotid artery and external jugular vein were cannulated for administration of anesthesia, blood exchange, laboratory analysis, and monitoring arterial blood pressure (Type514; Spacelabs, Hillsboro, OR). Catheterization and flap dissection were performed with the aid of an operating microscope at ×10 magnification (Wild; Heerbrugg, Switzerland). An island flap measuring 3 × 2 cm was dissected from the shaved and epilated back skin of the animal. The flap consisted of skin and a thin layer of panniculus carnosus muscle, and it was perfused by one vascular axis, which bifurcates into two equal-sized branches within the flap, each of them supplying a separate vascular territory. One of the branches was transected after being secured with microsurgical ligatures, thus rendering the corresponding vascular territory ischemic. This tissue was merely perfused by a collateral vasculature connecting the two vascular networks. During surgery, the flap was irrigated with 0.9% NaCl solution to prevent the flap from drying out. The animal was placed on a specially designed Plexiglas stage including a platform for fixation of the flap. During surgery, 4 mg papaverine hydrochloride (Sigma Chemical, St. Louis, MO) dissolved in 1 ml physiological saline solution were applied to the pedicle by a soaked cotton tip to prevent vascular spasm.

Vesicle solutions. The vesicles were prepared as previously reported (27, 28). They consisted of a phospholipid bilayer membrane coated with polyethylene glycol encapsulating either physiological saline solution (V) or isolated and purified human hemoglobin (HbV). The sizes of V and HbV were 274 ± 32 and 253 ± 63 nm, respectively. The Hb concentration inside the HbV was ~35 g/dl, and its P_{50} was 9 mmHg, which was calculated from the O_2 equilibrium curve measured with a Hemox Analyzer (TCS Medical Products) at 37°C (33). The vesicles were suspended in a solution with a final HES concentration of 6%.

Laboratory analysis. Blood samples were collected in 40-μl heparin-washed microtubes for measurement of total Hb concentration and arterial blood gases with the use of the Radiometer ABL 625 system (Radiometer; Copenhagen, Denmark). By validating this system, we have found that the vesicle-bound hemoglobin concentration may be overestimated by maximally 10%, whereas the results were not affected by the lipid concentrations present in our study. Hematocrit was determined by centrifugation. The colloid osmotic pressure of the diluents was measured with a colloid osmometer (model 4420; Wescor, Logan, UT) with a 30-kDa cutoff membrane. The viscosity was measured with a cone-plate viscometer (PVII+; Brookfield Engineering, Middleboro, MA) or a capillary rheometer (Anton Parr DCS 300; Parr Physica, Graz, Austria) at 37°C. Viscosities of blood and plasma were measured 4 h after hemodilution with a Höppler-type viscosimeter (HAAKE Messtechnik, Karlsruhe, Germany). The physicochemical characteristics of the solutions are summarized in Table 1. Oxygen content (ml/dl) in the carotid artery was calculated according to the equation

$$[O_2] = 1.34 \cdot \{([Hb_{RBC}] \cdot So_{2RBC}) + ([Hb_{HbV}] \cdot So_{2HbV})\}, \quad (1)$$

where 1.34 corresponds to the amount of oxygen (given in milliliters) bound to 1 g of Hb at 100% saturation. So_2 is the fractional oxygen saturation of red blood cells (RBCs) and HbV, which was derived from Po_2 by using the oxygen dissociation curves of the two hemoglobins (29).

Microhemodynamic measurements. Investigations were performed with the use of an intravital microscope (Axioplan 1; Zeiss, Jena, Germany). Microscopic images were captured by a television camera (intensified charge-coupled device camera; Kappa Messtechnik, Gleichen, Germany), recorded on video (50 Hz; Panasonic, Osaka, Japan), and displayed on a television screen for subsequent off-line analysis (Trinitron PVM-1454QM; Sony, Tokyo, Japan). The preparation was observed visually with a ×40 objective with a numerical aperture of 0.75, which resulted in a theoretical resolution of ~300 nm and a total optical magnification of ×909 on the video monitor, where 1 pixel corresponded to 264 nm in the tissue. The microvessels were classified according to physiological and anatomical features into conduit arterioles (connections to each other), end arterioles, and small venules (10, 12). The vessels were chosen for examination according to their optical clarity. The intraluminal microvascular diameters were measured visually on the television screen with the use of 2% fluorescein isothiocyanate-labeled dextran (FITC dextran, molecular mass 150 kDa; Sigma Chemical, Buchs, Switzerland) injected intra-arterially (0.05 ml), an excitation filter (485–505 nm), a dichroic mirror (510 nm), and a barrier filter (530 nm). The capillary hemodynamics and macromolecular leakage were assessed with a computer-assisted image analysis system (CapImage; Zeintl Software, Heidelberg, Germany) (17). Capillary diameters were obtained from the averages of five consecutive measurements. Because the capillary diameters measured with the present technique may possibly be underestimated because of the use of fluorescence microscopy and the optical properties of the microscope (22), the values were given in percentages of the mean obtained in the anatomically perfused tissue of the control group at baseline. FCD was defined as the length of RBC-perfused capillaries per observation field and expressed in centimeters per square centimeters. The product of RBC velocity and FCD was taken as an index reflecting the perfusion of the tissue with RBCs. The endothelial integrity was assessed by measuring macromolecular leakage (18). This was achieved by densitometric analysis of the fluorescence of FITC dextran 10 min after its injection. Macromolecular leakage was expressed by the ratio of fluorescence obtained in the interstitial space versus capillary fluorescence.

Table 1. *Physicochemical characteristics of hamster blood and diluents*

	Hamster Blood	Hamster Plasma	HES	V-HES	HbV-HES
[Hb], g/dl	18	0	0	0	7.5
[metHb], %					<3
[Lipid], g/dl				4.4	4.2
Oncotic pressure, mmHg		18	36	36	36
Viscosity of solution, cP	4.5	1.2	1.9	11.5	11.5
Plasma viscosity 4 h after exchange transfusion, cP		1.34 ± 0.03	1.31 ± 0.06	1.74 ± 0.13*	1.67 ± 0.12*

Values are means ± SD. HES, 6% hydroxyethyl starch; V-HES and HbV-HES, vesicles with and without hemoglobin suspended in HES, respectively; [Hb], hemoglobin concentration; [metHb], methemoglobin concentration. [Hb] was measured by a cyanomethemoglobin method, and [lipid] was measured with enzymatic method with use of phospholipase D. Viscosity of solutions was measured at 37°C and at 150 s^{-1}; plasma viscosity was measured at 25°C. *$P <$ 0.01 vs. hamster plasma and HES.

Tissue oxygen tension. Partial tissue oxygen tension was assessed with combined bare fiber probes with a tip diameter of 450 μm (Oxylite probes; Oxford Optronix, Oxford, UK). The sensitive tip of the oxygen probe (100-μm diameter) consists of ruthenium-III-(Tris)-chloride, which measures P_{O_2} by fluorescence quenching of the dye. A T-type thermocouple was attached to the probe, which was coated with a biocompatible sleeve of polyurethane. According to the manufacturer, the bare fiber probe provides resolutions of <1 mmHg and 0.1°C for partial oxygen tension and temperature, respectively, and the sampling area of the oxygen sensors is 0.25–0.35 mm^3. The probes were inserted into the subcutaneous tissue in the middle of each vascular territory under visual microscopic control. Care was taken to place the probes in such a way that no arterioles or large venules lay within the sampling area.

Tissue viability. The occurrence of apoptosis was assessed with the transferase-mediated dUTP nick end-labeling (TUNEL) assay (In Situ Cell Death Detection Kit, tetramethylrhodamine red; Roche Diagnostics, Rotkreuz, Switzerland) (1). All steps were performed according to the supplier's instructions. Tissue samples were obtained from the middle of each vascular territory. The samples were transferred to gelatinized microslides and air-dried overnight at 37°C. The sections were dewaxed in xylene (three changes), rehydrated in ethanol, and rinsed in Tris-buffered saline [50 mM Tris·NaCl, pH 7.4, containing 100 mM sodium chloride (two changes)], and then incubated in 20 μg/ml proteinase K for 15 min at room temperature. Endogenous peroxidase activity was suppressed by treatment with 0.3% hydrogen peroxide for 10 min. The sections were then incubated with terminal deoxynucleotidyl transferase enzyme for 1 h at 37°C followed by peroxidase-conjugated anti-digoxigenin antibody for 30 min at room temperature. The reaction was visualized by diaminobenzidine substrate for 8 min at room temperature. Thereafter, the sections were washed three times with Tris-buffered saline. The labeled DNA fragments were visualized by incubating the sections with tetramethylrhodamine used as a fluorescence marker, and the sections were examined with a fluorescence microscope (Leica DM/RB; Leica Microsystems, Wetzlar, Germany). Data were given as the averages of fluorescent cells counted in five randomly selected visual fields (0.5 × 0.5 mm) for the dermis and epidermis separately. Sebaceous glands and hair follicles were identified and excluded from the cell counts because of their consistently high apoptosis rate.

Protocol. The animals were kept under light anesthesia with a continuous infusion of 50 mg/ml pentobarbital sodium given at a rate of ~0.5 $mg \cdot min^{-1} \cdot kg$ body wt^{-1} throughout the experiment. The depth of anesthesia was regulated by tolerance of a noxious reflex due to pinching of the hind paw but no nonaversive reflexes (palpebral, corneal, and jaw reflex) (10). A constant temperature in the animal and flap preparation was maintained by means of a heating pad and by keeping room temperature at 28°C.

Baseline values were obtained after a postoperative period of 1 h had elapsed for stabilization. Thereafter, one-third of the total blood volume was exchanged with HES or the vesicle solutions. This was achieved by simultaneous blood withdrawal via the carotid catheter and infusion via the jugular catheter over 15 min. Measurements were taken hourly until 4 h after hemodilution, and tissue samples for immunohistochemical analysis were taken after 5 h.

Exclusion criteria were abnormalities of the vascular anatomy, insufficient optical clarity, mean arterial pressure <60 mmHg, and systemic arterial pH, P_{O_2}, and P_{CO_2} outside the normal ranges at baseline (7.19–7.29, 35–55, and 45–65 mmHg, respectively).

The animals were euthanized with an overdose of pentobarbital sodium at the end of the experiment.

Statistical analysis. The InStat version 3 program (Graph Pad Software; San Diego, CA) was utilized for statistical analysis. The data were presented as means ± SD. The time-related differences between repeat measurements were assessed by the paired ANOVA, followed by Dunnett's posttest. The differences between groups were assessed by the unpaired ANOVA, followed by Tukey's posttest. If only two sets of data were to be compared, paired (repeat measurements) and unpaired (differences between groups) *t*-tests were used. A value of $P < 0.05$ was taken to represent statistical significance.

RESULTS

Six animals did not fulfill the inclusion criteria and were excluded from this study, thus resulting in sample sizes of $n = 11$ for control, $n = 11$ for HES, $n = 9$ for V-HES, and $n = 11$ for HbV-HES.

The systemic data are summarized in Table 2. Similar hematocrits were obtained in all hemodiluted animals. The blood exchange reduced mean total Hb concentration to 10.4 and 10.1 g/dl for HES and V-HES, respectively, but only to 13.0 g/dl if HbV was added ($P < 0.01$ vs. other groups). Hemodilution increased arterial P_{O_2} to mean values of 58–61 mmHg ($P < 0.01$ vs. baseline) and decreased P_{CO_2} to 40–41 mmHg ($P < 0.05$), whereas pH remained virtually unchanged. Compared with the control animals, plasma viscosity was increased from 1.34 to ~1.7 cP after hemodilution with both vesicle solutions ($P < 0.01$ vs. control) but not with HES (Table 1).

Hemodilution resulted in an arterial oxygen content decrease from ~18 to 12.8 ± 1.5 ml/dl for HES and 12.6 ± 1.3 ml/dl for V-HES (both $P < 0.01$) after 4 h, whereas this reduction of oxygen-carrying capacity was significantly attenuated by adding HbV to the diluent (15.7 ± 1.2 ml/dl; $P < 0.01$ vs. baseline and other groups) (Fig. 1).

Table 2. *Systemic and laboratory data at baseline and 1 and 4 h after blood exchange*

	Baseline	1 h	4 h
MAP, mmHg			
Control	109±5	104±8	101±7
HES	105±8	107±5	99±2
V-HES	107±5	109±5	102±6
HbV-HES	105±5	107±5	103±3
Hematocrit			
Control	0.55±0.03	0.55±0.03	0.53±0.03
HES	0.57±0.03	0.33±0.03[b,d]	0.33±0.03[b,d]
V-HES	0.57±0.02	0.32±0.02[b,d]	0.32±0.01[b,d]
HbV-HES	0.56±0.02	0.33±0.02[b,d]	0.33±0.02[b,d]
Total Hb concentration, g/dl			
Control	18.0±1.1	18.0±1.4	17.2±1.1
HES	17.7±1.2	10.4±0.8[b,d]	11.2±0.8[b,d]
V-HES	17.8±1.3	10.1±0.3[b,d]	10.7±0.5[b,d]
HbV-HES	17.9±0.9	13.0±0.4[b,e]	13.2±0.7[b,e]
P_{O_2}, mmHg			
Control	43±3	44±6	49±8
HES	42±5	52±9[a]	59±12[b]
V-HES	40±8	52±8[a]	61±15[b]
HbV-HES	44±6	57±8[b,c]	58±10[b]
P_{CO_2}, mmHg			
Control	53±6	52±3	48±6
HES	52±4	48±5	41±7[a]
V-HES	51±6	43±8[a,c]	40±11[a]
HbV-HES	51±7	43±8[a,c]	41±6[a]
pH			
Control	7.34±0.04	7.34±0.05	7.36±0.05
HES	7.35±0.05	7.39±0.05	7.39±0.07
V-HES	7.33±0.05	7.38±0.06	7.37±0.08
HbV-HES	7.34±0.06	7.37±0.06	7.34±0.04

Values are means ± SD. MAP, mean arterial pressure. [a]$P < 0.05$ and [b]$P < 0.01$ vs. baseline; [c]$P < 0.05$ and [d]$P < 0.01$ vs. control; [e]$P < 0.01$ vs. other groups.

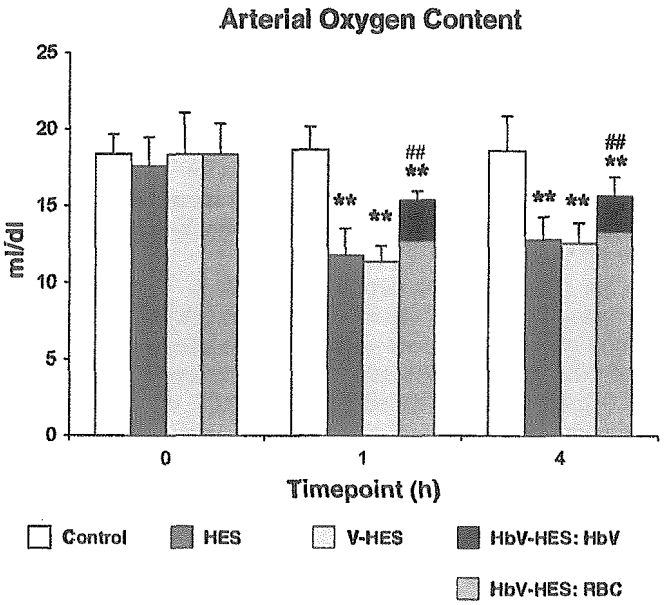

Fig. 1. Oxygen content in carotid artery at baseline and 1 and 4 h after hemodilution with 6% hydroxyethyl starch (HES) and vesicles with (HbV-HES) and without (V-HES) Hb suspended in HES, including relative contribution of red blood cells (RBCs) and HbV. Data are given as percentages of baseline and represent means ± SD. $^{**}P < 0.01$ vs. baseline; $^{\#\#}P < 0.01$ vs. other groups.

At baseline, the microvascular diameters were 42 ± 17 μm for conduit arterioles, 10.6 ± 3.5 μm for end arterioles, and 88 ± 14 μm for venules. In both flap areas and in all groups, the diameters were similar at baseline and they remained virtually unchanged throughout the experiments.

The behavior of the capillary hemodynamics in both parts of the flap is shown in Fig. 2. At baseline, the capillaries in the ischemic tissue were significantly wider than the anatomically perfused capillaries (means of 3.31–3.33 vs. 2.79–2.82 μm; $P < 0.01$). In the control group, the capillaries further dilated over time in both the anatomically perfused and the ischemic tissue by 25% and 9%, respectively (both $P < 0.01$). This time-related dilation was significantly attenuated in all hemodiluted animals ($P < 0.01$ vs. control), the most pronounced after HbV-HES, which resulted in a reduction of capillary diameter in the ischemic tissue to values close to baseline values obtained in the anatomically perfused tissue (2.85 ± 0.03 μm; $P < 0.01$ vs. baseline and other groups). The induction of ischemia reduced capillary RBC velocity by ~60% ($P < 0.01$). Hemodilution increased RBC velocity by ~50% in the anatomically perfused tissue and ~150% in the ischemic tissue (both $P < 0.01$ vs. baseline and control) for all diluents, whereas RBC velocity further declined in the ischemic tissue of the control animals over time by 67% ($P < 0.01$). In the ischemic tissue, baseline FCD was ~50% lower than in the anatomically perfused tissue ($P < 0.01$). In the control group, FCD decreased to 85% of baseline in the anatomically perfused tissue and to 69% in the ischemic tissue over time (both $P < 0.01$), whereas hemodilution kept FCD at baseline levels in the anatomically perfused tissue ($P < 0.01$ vs. control) and increased FCD in the ischemic tissue by 31% after HES ($P < 0.01$ vs. other groups), 66% after V-HES, and 62% after HbV-HES (all $P < 0.01$ vs. baseline). At baseline, the calculated RBC perfusion index in the ischemic tissue was reduced to ~20% of the value obtained in the anatomically perfused tissue ($P < 0.01$), and it was further decreased in both tissues of the control animals over time ($P < 0.01$). Hemodilution raised the RBC perfusion index by ~50% in the anatomically perfused tissue, independently of the diluent given ($P < 0.01$ vs. baseline and control), and by 186% after HES ($P < 0.01$ vs. other groups), 330% after V-HES, and 316% after HbV-HES in the ischemic tissue (all $P < 0.01$ vs. baseline and control; P = not significant between vesicle groups).

The baseline macromolecular leakage was slightly increased in the ischemic tissue compared with the anatomically perfused part (not significant; Fig. 3). In the control and HES groups, macromolecular leakage was increased by 20–30% in both parts of the flap over time ($P < 0.01$ for anatomical; $P < 0.05$ for ischemic), whereas it remained virtually unchanged after hemodilution with the vesicle solutions ($P < 0.01$ vs. control and HES).

The baseline mean Po_2 ranged from 22.7 to 25.2 mmHg in the anatomically perfused tissue and was significantly reduced in the ischemic tissue to 10.2–10.8 mmHg ($P < 0.01$; Fig. 4). The values remained at baseline levels in both parts of the flap and in all groups except for HbV-HES, which led to a significant Po_2 increase to 16.0 ± 1.8 mmHg in the ischemic tissue ($P < 0.01$ vs. baseline and other groups).

A massive accumulation of TUNEL-positive nuclei was observed in the ischemic tissue of untreated animals (Fig. 5). Compared with the anatomically perfused tissue, a 2-fold increase was counted in the dermis and a 1.5-fold increase in the epidermis (Fig. 6; both $P < 0.01$), which were both partly attenuated by diluting the animals with HES and V-HES (both $P < 0.01$ vs. control) and completely abolished after HbV-HES, which also revealed significantly lower counts in the anatomically perfused tissue ($P < 0.01$ vs. other groups).

DISCUSSION

This study was designed to determine the relevance of Hb supplemented as an oxygen carrier to a solution used for isovolemic hemodilution with the scope of improving oxygenation in critically ischemic tissue, as previously described (8, 12). This was made possible by direct comparison of the oxygen-carrying solution with a solution void of oxygen carriers but with otherwise absolutely identical physicochemical properties, a constellation that, to our knowledge, has not yet been investigated. Our findings revealed that the presence of Hb in the vesicles administered in the course of isovolemic hemodilution was essential to significantly attenuate both hypoxia and subsequent cell death in the critically ischemic tissue, which were restored to values in the range of those found in the anatomically perfused tissue.

However, some benefit in tissue survival could also be obtained with the diluents void of oxygen carriers, which was related to a substantial improvement in all capillary hemodynamic parameters, and which was more pronounced in the compromised microcirculation in the ischemic tissue. The level of hemodilution we chose is considered to yield the maximal RBC flux at the capillary level (20). However, compared with HES, the improvement in capillary hemodynamics in the ischemic tissue was further enhanced by adding vesicles to the solution, which resulted in a significant increase in plasma

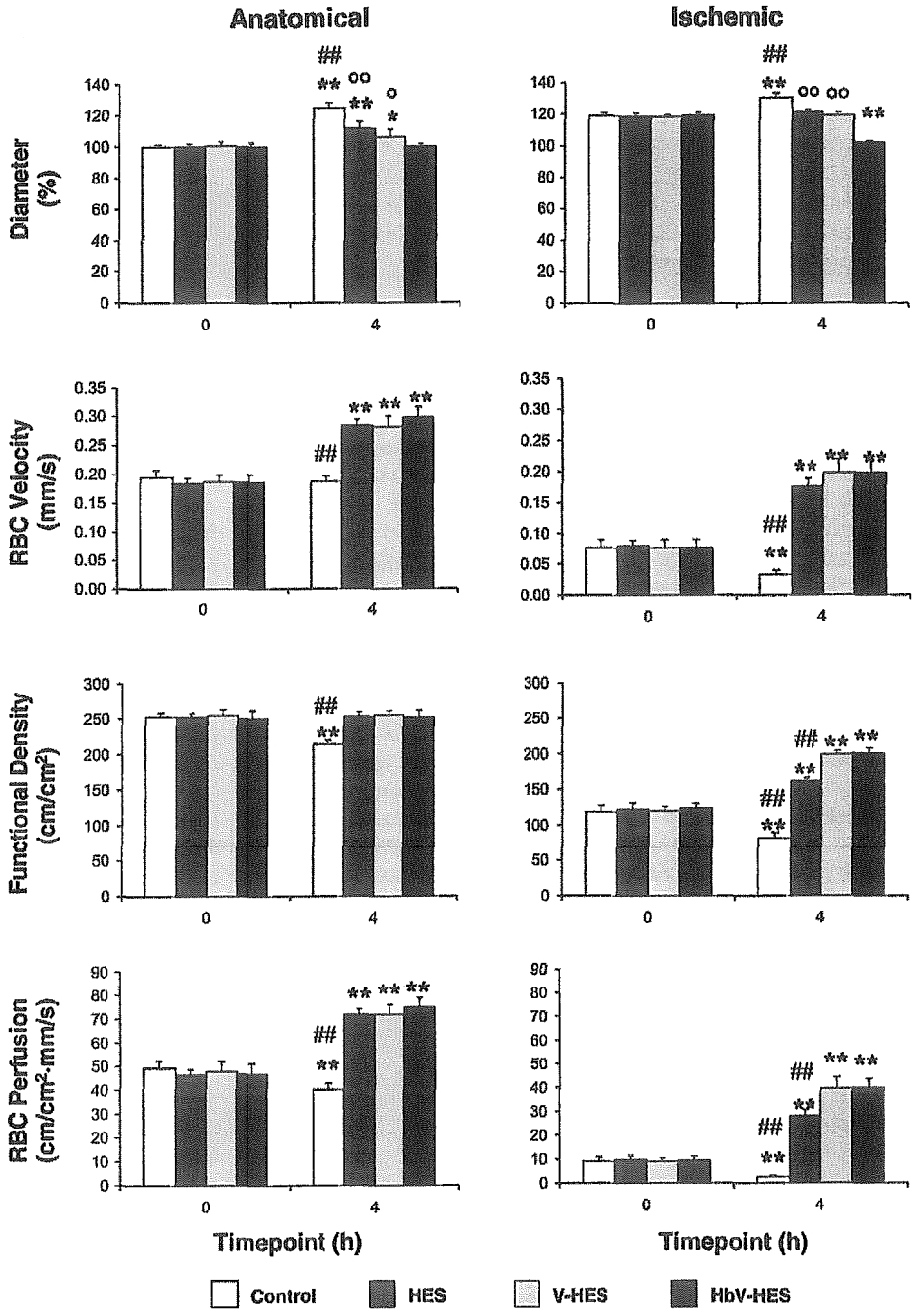

Fig. 2. Capillary hemodynamics in anatomically perfused and ischemic tissues at baseline and 4 h after hemodilution with 6% HES, HbV-HES, and V-HES. Data represent means ± SD. Values for capillary diameter were expressed in percentages of mean in anatomically perfused tissue of control animals at baseline. $*P < 0.05$, $**P < 0.01$ vs. baseline; $\#\#P < 0.01$ vs. other groups; $^{\circ}P < 0.05$, $^{\circ\circ}P < 0.01$ vs. HbV-HES.

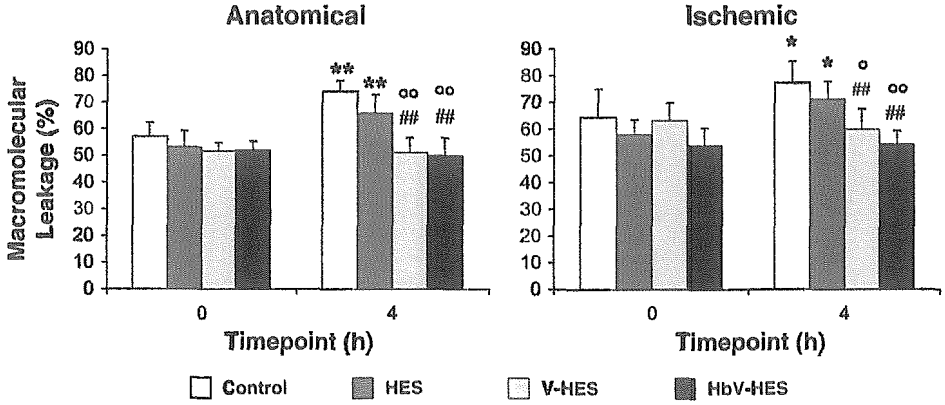

Fig. 3. Macromolecular leakage in anatomically perfused and ischemic tissues at baseline and 4 h after hemodilution with 6% HES, HbV-HES, and V-HES. Data represent means ± SD. $*P < 0.05$, $**P < 0.01$ vs. baseline; $\#\#P < 0.01$ vs. control; $^{\circ}P < 0.05$, $^{\circ\circ}P < 0.01$ vs. HES.

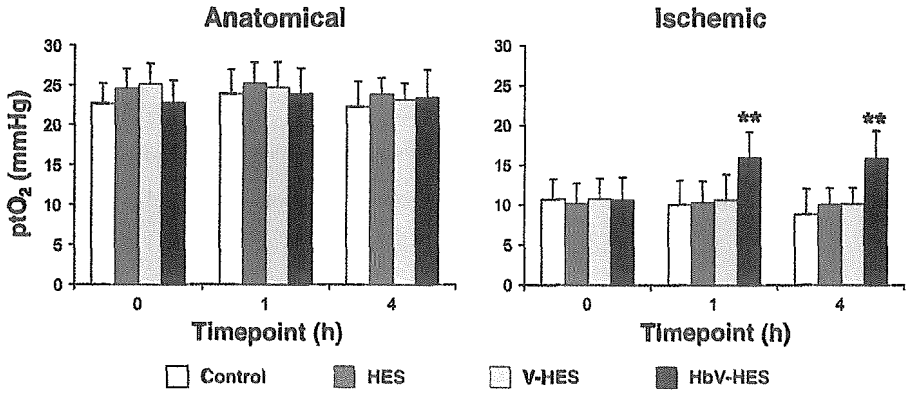

Fig. 4. Partial tissue oxygen tension (P_tO_2) in anatomically perfused and ischemic tissues at baseline and 1 and 4 h after hemodilution with 6% hydroxyethyl starch (HES), HbV-HES, and V-HES. Data represent means ± SD. $^{**}P < 0.01$ vs. baseline and other groups.

viscosity. A dependency of FCD on plasma viscosity has been described for conditions of severe hemodilution (2, 3, 33), which has been ascribed to shear stress-induced, nitric oxide-mediated arteriolar vasodilation being required to maintain capillary pressurization (2, 3, 9). However, during the moderate hemodilution applied in the present study, no such arteriolar vasodilation could be observed, which calls for alternative explanations not only for the behavior of FCD but also of capillary RBC velocity and perfusion.

One interpretation may be found in the changes in macromolecular leakage. This parameter allows for a quantitative assessment of capillary leakage, which is an early sign of inflammation appearing in the course of compromised microcirculation such as that due to trauma (31), hemorrhagic shock (5), or ischemia-reperfusion injury (18), and which is paralleled by the activation of the leukocyte-endothelium interaction particularly in the postcapillary venules. Leukocyte adherence, being an early step in this cascade of events, may augment resistance in this vascular segment considerably and thus impair capillary hemodynamics in critically perfused tissues (19). Compared with both the control group and the HES group, macromolecular leakage was significantly reduced in the animals receiving vesicles. Therefore, it may be postulated that the beneficial effect of the vesicles on the capillary hemodynamics was related to a reduction of postcapillary resistance in terms of blunting leukocyte adherence. The capability of leukocytes to adhere to the endothelial wall may be diminished by increasing shear stress (21), which is proportional to linear flow velocity and viscosity of the plasma and inversely proportional to vascular diameter. Provided that our data on plasma viscosity and capillary hemodynamics may be extrapolated to the conditions in the ischemic postcapillary

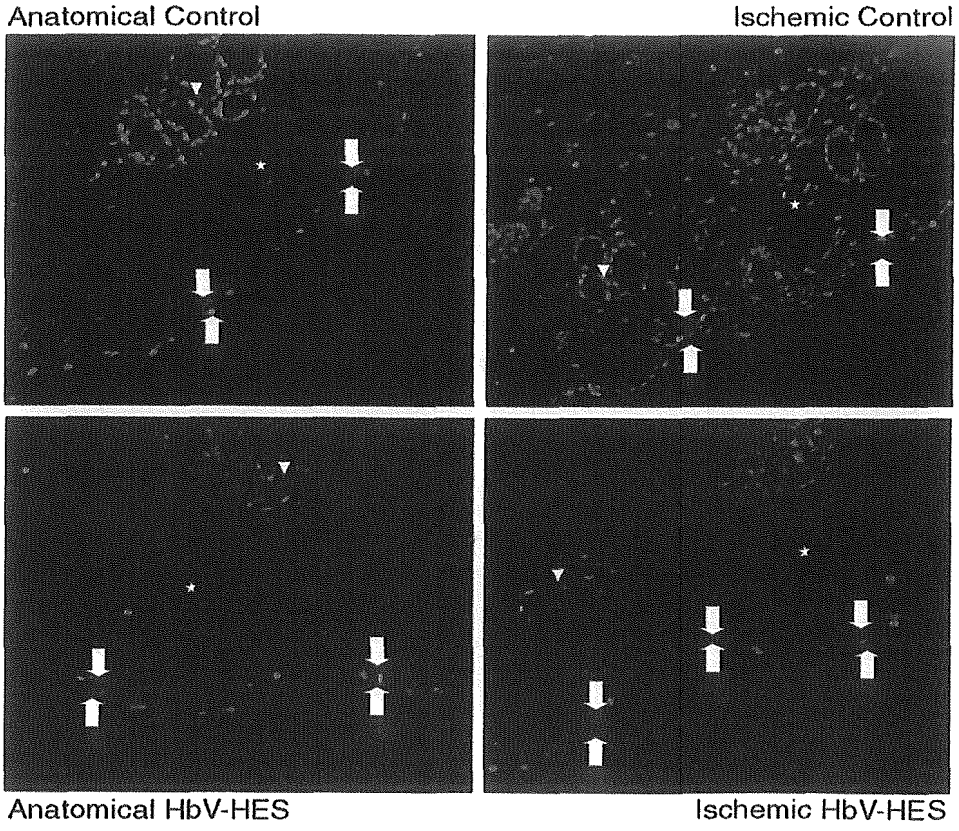

Fig. 5. Transferase-mediated dUTP nick-end labeling (TUNEL) assay of apoptotic cells in anatomically perfused and ischemic tissues 5 h after completion of surgery and 4 h after hemodilution with HbV-HES. Note massive accumulation of red-labeled apoptotic cells in both dermis (☆) and epidermis (arrows) of ischemic tissue and how apoptosis was reduced after hemodilution with HbV-HES. Hair follicles and sebaceous glands are shown (arrowheads).

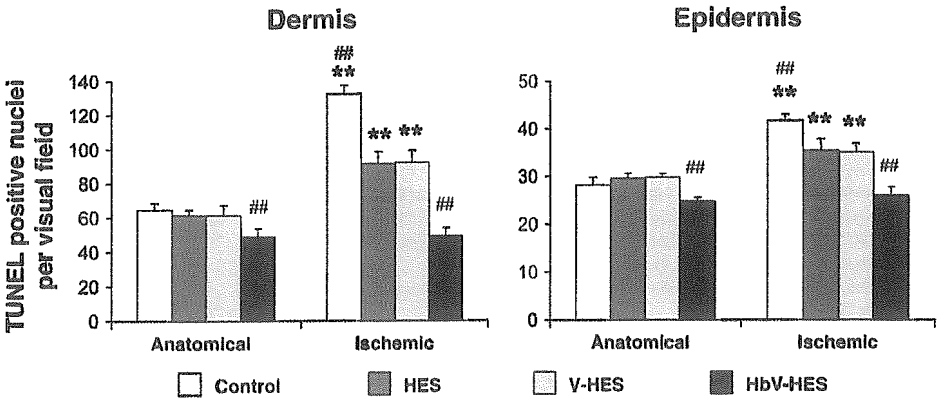

Fig. 6. Density of apoptotic cells in dermis and epidermis of anatomically perfused and ischemic tissues 5 h after completion of surgery and 4 h after hemodilution with 6% HES, HbV-HES, and V-HES. Data represent means ± SD. $^{**}P < 0.01$ vs. anatomically perfused tissue: $\#\#P < 0.01$ vs. other groups.

venules, hemodilution with the vesicle solutions would result in a significant shear stress increase in these vessels compared with baseline and HES, respectively. This mechanism may be of a particular importance in case of ischemia-reperfusion injury after reoxygenation of critically ischemic tissue (16), which may, at least partly, have taken place in the animals receiving HbVs, as evidenced by the improved partial tissue oxygen tension.

In the present preparation, macromolecular leakage appeared to be primarily related to the traumatization of the tissue as a consequence of its surgical manipulation (7), because similar values were obtained in both parts of the flap. However, it is conceivable that the ischemic tissue is more susceptible to changes in postcapillary resistance because of the diminished driving pressure in the collateralized arterioles that are nourished by connecting arterioles, in which perfusion pressures below 30 mmHg were measured, compared with ~45 mmHg in the arterioles feeding the anatomically perfused vasculature (3, 10). With regard to the postulated effect of the vesicles on the postcapillary resistance, this would explain why the vesicle-related improvement of capillary hemodynamics was restricted to the ischemic tissue. Moreover, the vesicle-related increase in capillary perfusion coincided with a decrease in capillary diameters. Given the assumption that the perfusion increase was caused by a reduction of upstream vascular resistance, this would have led to capillary dilation as a result of increased intraluminal capillary pressure (3), whereas intraluminal capillary pressure decreases if vascular resistance is diminished on the postcapillary level. Therefore, the inversely proportional behavior of capillary diameter and perfusion further supports our assumption that the microhemodynamic benefit obtained with the vesicle solutions was predominantly due to its reduction of postcapillary resistance.

Although all capillary hemodynamic parameters in the ischemic tissue were restored to values close to baseline in the anatomically perfused tissue in the V-HES group, this was not sufficient to attenuate hypoxia or hypoxia-induced apoptosis. This suggests that in this group, oxygen delivery to the ischemic tissue is reduced because of a lack of oxygen content in its collateralized, arteriolar inflow, a condition that was presumably circumvented by the presence of Hb in the vesicles because of various reasons. First, the HbVs contribute to a total Hb increase, thus resulting in an enhanced oxygen-carrying capacity not only in terms of arterial oxygen content but also in terms of additional capillary, HbV-related oxygen flow that is not included in the index used to express capillary perfusion in the present study. Second, the high oxygen affinity of the HbVs may have attenuated the unloading of oxygen in the upstream vasculature before reaching the collateralized arterioles, which has been estimated to be as much as 40–50% of the systemic arterial oxygen content (11, 30). This hypothesis is supported by both experimental (15, 25, 30) and theoretical (34) studies, which showed that oxygen delivery may be shifted to the downstream direction if oxygen carriers with high oxygen affinity were infused. Third, because of their small size, HbVs may perfuse capillaries in the compromised microcirculation that are no longer accessible by RBCs. Indeed, HbVs were observed in capillaries showing a cessation of RBC flux (29), which would virtually enhance the density of functional capillaries. Moreover, the occurrence of apoptosis leads to a reduction of oxygen consumption, thus raising partial tissue oxygen tension, provided oxygen delivery remains unchanged. Therefore, the partial tissue oxygen tension increase observed after HbV-HES may underestimate the improvement in oxygen delivery in comparison with the other groups.

In summary, on the basis of the unique constellation in which a HbV solution was compared with a nonoxygen-carrying vesicle solution with identical physicochemical properties, we conclude that the presence of Hb in the vesicles is necessary to obtain an essential improvement of oxygenation and survival in the critically ischemic flap tissue. However, the benefit may, to a certain extent, be ascribed to the rheological changes provided by the vesicles, presumably by reducing postcapillary vascular resistance.

ACKNOWLEDGMENTS

We greatly acknowledge Prof. S. Takeoka and Dr. K. Sou (Advanced Research Institute for Science and Engineering, Waseda University, Tokyo, Japan) for the preparation of the phospholipid vesicles, and Prof. A. C. Andres and V. Rohrbach (Department of Clinical Research, Inselspital University Hospital, Bern, Switzerland) for assistance in the immunohistochemical analysis.

GRANTS

This research was supported by the Swiss National Foundation for Scientific Research Grants 32–054092.98 and 32–065149.01 (to D. Erni) and 32–050771.97 (to M. Leunig), by the Department of Clinical Research, University of Berne, Switzerland, and by Health Sciences Research (Research on Regulatory Science Grant H16-IYAKU-069, 071) from the Ministry of Health, Labour and Welfare, Japan, and Grants-in-Aid for Scientific Research from the Japan Society for the Promotion of Science (B-16300162).

REFERENCES

1. **Ansari B, Coates PJ, Greenstein BD, and Hall PA.** In situ end-labeling detects DNA strand breaks in apoptosis and other physiological and pathological states. *J Pathol* 170: 1–8, 1993.
2. **Bertuglia S.** Increased viscosity is protective for arteriolar endothelium and microvascular perfusion during severe hemodilution in hamster cheek pouch. *Microvasc Res* 61: 56–63, 2001.
3. **Cabrales P, Tsai AG, and Intaglietta M.** Microvascular pressure and functional capillary density in extreme hemodilution with low- and high-viscosity dextran and a low-viscosity Hb-based O_2 carrier. *Am J Physiol Heart Circ Physiol* 287: H363–H373, 2004.
4. **Chang TM.** Artificial cells for cell and organ replacements. *Artif Organs* 28: 265–270, 2004.
5. **Childs EW, Udobi KF, and Hunter FA.** Hypothermia reduces microvascular permeability and reactive oxygen species expression after hemorrhagic shock. *J Trauma* 58: 271–277, 2005.
6. **Chowdary RP, Berkower AS, Moss ML, and Hugo NE.** Fluorocarbon enhancement of skin flap survival in rats. *Plast Reconstr Surg* 79: 98–101, 1987.
7. **Contaldo C, Plock JA, Djonov V, Leunig M, Banic A, and Erni D.** The influence of trauma and ischemia on carbohydrate metabolites monitored in hamster flap tissue. *Anesth Analg*: 817–822, 2005.
8. **Contaldo C, Schramm S, Wettstein R, Sakai H, Takeoka S, Tsuchida E, Leunig M, Banic A, and Erni D.** Improved oxygenation in ischemic hamster flap tissue is correlated with increasing hemodilution with Hb vesicles and their O_2 affinity. *Am J Physiol Heart Circ Physiol* 285: H1140–H1147, 2003.
9. **de Wit C, Schafer C, von Bismarck P, Bolz SS, and Pohl U.** Elevation of plasma viscosity induces sustained NO-mediated dilation in the hamster cremaster microcirculation in vivo. *Pflügers Arch* 434: 354–361, 1997.
10. **Erni D, Sakai H, Banic A, Tschopp H, and Intaglietta M.** Quantitative assessment of microhemodynamics in ischemic skin flap tissue by intravital microscopy. *Ann Plast Surg* 43: 405–415, 1999.
11. **Erni D, Sakai H, Tsai AG, Banic A, Sigurdsson GH, and Intaglietta M.** Haemodynamics and oxygen tension in the microcirculation of ischaemic skin flaps after neural blockade and haemodilution. *Br J Plast Surg* 52: 565–572, 1999.
12. **Erni D, Wettstein R, Schramm S, Contaldo C, Sakai H, Takeoka S, Tsuchida E, Leunig M, and Banic A.** Normovolemic hemodilution with Hb vesicle solution attenuates hypoxia in ischemic hamster flap tissue. *Am J Physiol Heart Circ Physiol* 284: H1702–H1709, 2003.
13. **Faithfull NS, Fennema M, and Erdmann W.** Protection against myocardial ischaemia by prior haemodilution with fluorocarbon emulsions. *Br J Anaesth* 60: 773–778, 1988.
14. **Fitzpatrick CM, Savage SA, Kerby JD, Clouse WD, and Kashyap VS.** Resuscitation with a blood substitute causes vasoconstriction without nitric oxide scavenging in a model of arterial hemorrhage. *J Am Coll Surg* 199: 693–701, 2004.
15. **Intaglietta M.** Microcirculatory basis for the design of artificial blood. *Microcirculation* 6: 247–258, 1999.
16. **Kajimura M, Ichikawa M, Sakai H, Takeoka S, Tsuchida E, and Suematsu M.** Real time imaging of anionic liposome during thrombus formation and acute inflammation in rats (Abstract). In: *2nd Japan-United Kingdom Platelet Conference, Oxford, UK, 2004*. London: Br Soc for Haemostasis and Thrombosis, 2004.
17. **Klyscz T, Jünger M, Jung F, and Zeintl H.** Cap image–A new kind of computer-assisted video image analysis system for dynamic capillary microscopy. *Biomed Tech* 42: 168–175, 1997.
18. **Menger MD, Pelikan S, Steiner D, and Mesmer K.** Microvascular ischemia-reperfusion injury in striated muscle: significance of "reflow paradox." *Am J Physiol Heart Circ Physiol* 263: H1901–H1906, 1992.
19. **Menger MD, Steiner D, and Messmer K.** Microvascular ischemia-reperfusion injury in striated muscle: significance of "no reflow." *Am J Physiol Heart Circ Physiol* 263: H1892–H1900, 1992.
20. **Mirhashemi S, Ertefai S, Messmer K, and Intaglietta M.** Model analysis of the enhancement of tissue oxygenation by hemodilution due to increased microvascular flow velocity. *Microvasc Res* 34: 290–301, 1987.
21. **Moazzam F, DeLano FA, Zweifach BW, and Schmid-Schönbein GW.** The leukocyte response to fluid stress. *Proc Natl Acad Sci USA* 94: 4825–4827, 1997.
22. **Piston DW.** Choosing objective lenses: the importance of numerical aperture and magnification in digital optical microscopy. *Biol Bull* 195: 1–4, 1998.
23. **Powanda DD and Chang TM.** Cross-linked polyhemoglobin-superoxide dismutase-catalase supplies oxygen without causing blood-brain barrier disruption or brain edema in a rat model of transient global brain ischemia-reperfusion. *Artif Cells Blood Substit Immobil Biotechnol* 30: 23–37, 2002.
24. **Premaratne S, Harada RN, Chun P, Suchiro A, and McNamara JJ.** Effect of perfluorocarbon exchange transfusion on reducing myocardial infarct size in a primate model of ischemia-reperfusion injury: a prospective, randomized study. *Surgery* 117: 670–676, 1995.
25. **Sakai H, Cabrales P, Tsai AG, Tsuchida E, and Intaglietta M.** Oxygen release from low and normal P_{50} Hb vesicles in transiently occluded arterioles of the hamster window model. *Am J Physiol Heart Circ Physiol* 288: H2897–H2903, 2005.
26. **Sakai H, Hara H, Yuasa M, Tsai AG, Takeoka S, Tsuchida E, and Intaglietta M.** Molecular dimensions of Hb-based O_2 carriers determine constriction of resistance arteries and hypertension. *Am J Physiol Heart Circ Physiol* 279: H908–H915, 2000.
27. **Sakai H, Masada Y, Horinouchi H, Ikeda E, Sou K, Takeoka S, Suematsu M, Takaori M, Kobayashi K, and Tsuchida E.** Physiological capacity of the reticuloendothelial system for the degradation of hemoglobin vesicles (artificial oxygen carriers) after massive intravenous doses by daily repeated infusions for 14 days. *J Pharmacol Exp Ther* 311: 874–884, 2004.
28. **Sakai H, Masada Y, Horinouchi H, Yamamoto M, Ikeda E, Takeoka S, Kobayashi K, and Tsuchida E.** Hemoglobin-vesicles suspended in recombinant human serum albumin for resuscitation from hemorrhagic shock in anesthetized rats. *Crit Care Med* 32: 539–545, 2004.
29. **Sakai H, Takeoka S, Wettstein R, Tsai AG, Intaglietta M, and Tsuchida E.** Systemic and microvascular responses to hemorrhagic shock and resuscitation with Hb vesicles. *Am J Physiol Heart Circ Physiol* 283: H1191–H1199, 2002.
30. **Sakai H, Tsai AG, Rohlfs RJ, Hara H, Takeoka S, Tsuchida E, and Intaglietta M.** Microvascular response to hemodilution with Hb vesicles as red blood cell substitutes: influence of O_2 affinity. *Am J Physiol Heart Circ Physiol* 276: H552–H562, 1999.
31. **Schaser KD, Vollmar B, Menger MD, Schewior L, Kroppenstedt SN, Raschke M, Lubbe As Haas NP, and Mittlmeier T.** In vivo analysis of microcirculation following closed soft-tissue injury. *J Orthop Res* 17: 678–685, 1999.
32. **Sutherland GR, Farrar JK, and Peerless SJ.** The effect of Fluosol-DA on oxygen availability in focal cerebral ischemia. *Stroke* 15: 829–835, 1984.
33. **Tsai AG, Friesenecker B, McCarthy M, Sakai H, and Intaglietta M.** Plasma viscosity regulates capillary perfusion during extreme hemodilution in hamster skinfold model. *Am J Physiol Heart Circ Physiol* 275: H2170–H2180, 1998.
34. **Vadapalli A, Goldman D, and Popel AS.** Calculations of oxygen transport by red blood cells and hemoglobin solutions in capillaries. *Artif Cells Blood Substitut Immobil Biotechnol* 30: 157–188, 2002.

Artificial Cells, Blood Substitutes, and Biotechnology, 33: 101–111, 2005

ISSN: 1073-1199 print/1532-4184 online
DOI: 10.1081/BIO-200055856

Taylor & Francis
Taylor & Francis Group

Effects of Hemoglobin Vesicles on Resting and Agonist-Stimulated Human Platelets In Vitro

Shinobu Wakamoto, Mitsuhiro Fujihara, Hideki Abe, Miki Yamaguchi, Hiroshi Azuma, and Hisami Ikeda
Japanese Red Cross, Hokkaido Red Cross Blood Center, Sapporo, Japan

Shinji Takeoka and Eishun Tsuchida
Department of Polymer Chemistry, Advanced Research Institute for Science and Engineering, Waseda University, Tokyo, Japan

Abstract: Hemoglobin vesicles (HbV) are artificial oxygen carriers that encapsulate a concentrated hemoglobin (Hb) solution with a phospholipid bilayer membrane. The oxygen transporting ability of HbV in vivo has been demonstrated by the transfusion of HbV into hemorrhagic shock rodent models. However, the compatibility of HbV with human blood cells must be evaluated. Preincubation of platelets with concentrations of 20% or 40% HbV had no effect on the binding of PAC-1, a monoclonal antibody that detects activation-dependent conformational changes in $\alpha_{IIb}\beta_3$ on platelets, or the surface expression of CD62P in whole blood. ADP-induced increases in PAC-1 binding were significantly enhanced by exposing the platelets to concentrations of either 20% or 40% HbV, whereas the ADP-induced increases in CD62P expression were not affected by HbV treatment at either concentration. Preincubation of platelet-rich plasma (PRP) with HbV minimally reduced the spontaneous release of TXB_2 and RANTES, but did not significantly affect the formation of TXB_2 or the release of RANTES and β-TG in platelets stimulated with ADP. Similarly, preincubation of PRP with HbV minimally reduced the spontaneous release of RANTES but did not significantly affect the formation of TXB_2 or the release of RANTES and β-TG in platelets stimulated with collagen, although collagen-induced serotonin release tended to decrease with HbV pretreatment. These data suggest that the exposure of human platelets to high concentrations of HbV (up to 40%) in vitro did not cause platelet activation and did not adversely affect the formation and secretion of prothrombotic substances or proinflammatory substances triggered by platelet agonists, although one of the earliest events in ADP-induced platelet activation was slightly potentiated by HbV pretreatment at the doses tested. Taken together,

Address correspondence to Mitsuhiro Fujihara, Japanese Red Cross, Hokkaido Red Cross Blood Center, Sapporo 063-0002, Japan. E-mail: Fujihara@hokkaido.bc.jrc.or.jp

these results imply that HbV, at concentrations of up to 40%, do not have any aberrant interactions with either unstimulated or agonist-induced platelets.

INTRODUCTION

Vigorous efforts have been made to develop hemoglobin (Hb)-based oxygen carriers (HBOCs) for use as red blood cell substitutes [1], and some of these carriers are now in the final stages of clinical trials [2–4]. HBOCs offer several potential benefits for red blood cell transfusion applications, including the absence of blood-type antigens and infectious viruses and the ability to be stably stored for long time periods [5]. HBOCs can be categorized into two types: acellular modified Hb molecules and cellular liposome-encapsulated Hb, or Hb vesicles (HbV) [6]. Acellular modified Hb molecules are composed of intramolecularly cross-linked Hb, recombinant cross-linked Hb, polymerized Hb, or intramolecularly polymer-conjugated Hb. An acellular polymerized bovine Hb has already been used in clinical practice in South Africa.

Cellular HbV have a phospholipid vesicle structure and contain concentrated Hb molecules, similar to actual red blood cells [7–11]. Although HbV have not been clinically tested, the oxygen transporting abilities of HbV have been shown to be sufficient using a 40% exchange transfusion with HbV suspended in saline [8] and a 90% exchange transfusion with HbV in the presence of albumin as a plasma expander in rats [7]. Surface modification of HbV with poly(ethyleneglycol)-phospatidylethanolamine reduced the viscosity by suppressing inter-vesicular aggregation, allowing prompt blood circulation in vivo [9]. A sufficient O_2 transporting ability, comparable with that of blood, was also established in another model [11], and the prompt metabolism of HbV in the reticulo-endothelial system has been demonstrated [10].

The biocompatibility of HbV is an important factor for the clinical use of these materials. The administration of HbV could lead to interactions with blood cells, including platelets. Circulating platelets bind to the subendothelial matrix of injured vessels and subsequently become activated, resulting in the release or the expression of components in their intracellular granules and the formation of metabolic products. These products include prothrombotic substances (e.g., adenine nucleotides, thromboxane A_2 [TXA_2], serotonin, and CD62P) [12] and an array of potent proinflammatory chemokines (e.g., RANTES, MIP-1) [13]. Prothrombotic substances function as agonists for the recruitment of additional platelets into the evolving thrombus. Chemokines released from the activated platelets trigger the recruitment of leukocytes into the evolving thrombus and play a large role in the initiation and perpetuation of inflammatory responses. Platelet activation is apparently necessary to prevent bleeding in vivo; however, nonphysiological activation leads to pathological thrombosis and the

modulation of inflammatory responses. With this in mind, the biocompatibility of HbV and human platelets was evaluated by examining the effect of HbV on CD62P expression and the binding of activation–dependent $\alpha_{IIb}\beta_3$ antibody PAC-1 to platelets in the presence or absence of agonists in vitro; these two markers are the most frequently used markers of platelet activation. We also studied the effects of HbV on the secretion of other substances (i.e., serotonin, RANTES, and β-thromboglobulin [β-TG]) and the formation of thromboxane B_2 (TXB_2), a metabolite of TXA_2.

MATERIALS AND METHODS

HbV

HbV suspended in phosphate buffered saline were prepared as previously described [14]. The encapsulated carbonylhemoglobin contained pyridoxal 5′-phosphate (PLP) at a molar ratio of [Hb]/[PLP] = 1/2.5 as an allosteric effector and 5 mM of DL-homocysteine. The lipid bilayer was composed of 1,2-dipalmitoyl-sn-glycero-3-phosphatidylcholine, cholesterol, 1,5-dipalmitoyl-L-glutamate-*N*-succinic acid, and polyethyleneglycol-1, 2-distearyl-*sn*-glycero-3-phosphatidylethanolamine-*N*-[poly (ethylene glycol) (5,000)] at a molar ratio of 5:5:1:0.033. The Hb concentration of the HbV dispersion was adjusted to 10 g/dl. The HbV particle size was nearly 240 ± 60 nm in diameter.

Determination of CD62P and PAC-1 Expression by Flow Cytometry

The expression of CD62P and PAC-1 on platelets was measured as described previously, with slight modifications [15, 16]. Citrated whole blood was obtained from unselected healthy subjects. Whole blood (520 μl) was incubated with 480 μl of HbV or empty liposomes (at concentrations of 0%, 20%, or 40%) at 37°C for 60 minutes. After incubation, the reaction mixture was diluted to 1/5.4 with Hepes-Tyrode's buffer (KCl, 2 mM; NaCl, 127 mM; NaH_2PO_4, 0.5 mM; glucose, 5.6 mM; $NaHCO_3$, 12 mM; HEPES, 5 mM; 0.35% BSA; pH 7.3). Eighteen microliters of the diluted reaction mixture was added to 18 μl of a cocktail of FITC-conjugated PAC-1, PE-conjugated anti-CD62P and PerCP-conjugated anti-CD42a. FITC-conjugated anti-mouse IgM, PE-conjugated anti-mouse IgG, and PerCP-conjugated anti-mouse IgG were used as negative controls. All antibodies were purchased from BD bioscience-Pharmingen, San Jose, CA. The reaction mixture was then incubated with 4 μl of ADP (final concentration of 0, 0.05, 0.1, 0.5, 5, or 10 μM) for 20 minutes at room temperature in the dark. After incubation, the platelet suspension was fixed with 500 μl of paraformaldehyde (final concentration, 1%) and washed once with PBS. Finally, the platelets were resuspended in

500 μL of PBS. The samples were analyzed by flow cytometry (LSR, Becton-Dickinson, San Jose, CA). Fluorescence data from 10,000 platelet events were collected in logarithmic mode. The platelet population was identified by the number of CD42a-positive events.

Assay of Mediator Release

The platelet mediator release assay was carried out as described by Santos et al. [17], with slight modifications. Platelet-rich plasma (PRP) was obtained from citrated venous blood of unselected healthy subjects by centrifugation (140 g, 15 minutes, 22°C), and 600 μl of PRP (final concentration, 1.7×10^8/ml) was incubated with 400 μl of HbV (0%, 20%, or 40%) at 37°C for 60 minutes. After incubation, the mixture was divided into two 480 μl aliquots. For the collagen-induced platelet release reaction, the mixture was activated with 20 μl of collagen (final concentration, 1 μg/ml) (NYCOMED ARZNEIMITTEL BMBH, Germany) or buffer at 37°C for 5 minutes. For the ADP-induced platelet release reaction, the mixture was activated with 20 μl of ADP (final concentration, 2 μM) (SIGMA) or PBS at room temperature for 20 minutes. After incubation, the tube was centrifuged at 10,000 g for 1 minute. The cell-free supernatant was then transferred to another tube and centrifuged at 10,000 g for 30 minutes. The cell-free supernatant was stored at −20°C until the measurement of platelet release. Commercially available enzyme-linked immunosorbent assays (ELISAs) were used to measure the levels of RANTES (R&D Systems, Minneapolis, MN), serotonin (ICN Biomedicals Inc., Costa Mesa, CA) and TXB_2 (Cayman Chemical Company, Ann Arbor, MI) in duplicate experiments, according to the manufacturers' recommendations. Enzyme immunoassays were used to measure the levels of β-TG (Asserachrom β-TG, Roche Diagnostics, Tokyo, Japan).

Statistical Analysis

A two-way repeated measures ANOVA with Bonferroni correction was used for multiple comparisons of mediator levels and surface marker levels among different concentrations of HbV. A p value <0.05 was considered to indicate a significant difference.

RESULTS

Effect of HbV on the Binding of PAC-1 and the Expression of CD62P on Resting and ADP-stimulated Platelets In Vitro in Whole Blood

First, the effect of HbV on the binding of PAC-1 to platelets and the surface expression of CD62P on platelets with or without ADP stimulation

was examined in a whole blood environment in vitro. Without ADP stimulation, PAC-1 binding to platelets was discernible. Preincubation of whole blood with 20% or 40% HbV alone did not cause a significant difference in PAC-1 binding to the platelets. Stimulation of platelets with varying concentrations of ADP caused a gradual increase in the percentage of PAC-1 positive cells (Fig. 1A). Preincubation of whole blood with 20% or 40% HbV resulted in a slight, but significant, enhancement in the percentage of PAC-1 positive cells, compared to the results of comparable experiments without HbV, at ADP concentrations ranging from 0.05 μM to 5 μM (Fig. 1A).

Unstimulated platelets showed only a slight expression of CD62P, regardless of HbV treatment (Fig. 1B). The treatment of platelets with varying concentrations of ADP also led to gradual increases in the percentage of CD62P-positive cells, but preincubation of whole blood with 20% or 40% HbV did not affect the ADP-induced increase in the percentage of CD62P-positive cells (Fig. 1B).

Effect of HbV on Secretion of Platelet-derived Mediators in Resting and ADP-stimulated Platelets In Vitro

Next, the effect of HbV on the release of mediators from platelets stimulated with or without a submaximal dose of ADP, a weak platelet

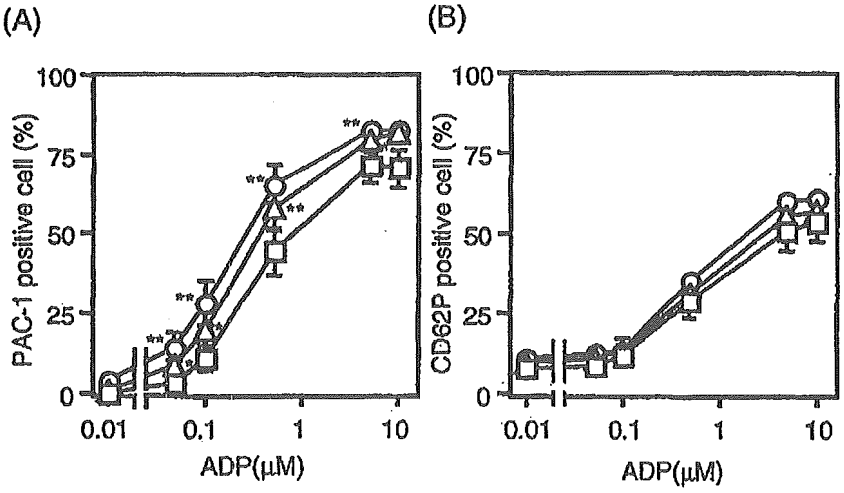

Figure 1. Effect of HbV on platelet surface activation markers. (A) PAC-1 binding to platelets and (B) CD62P expression on platelets. Whole blood was incubated with HbV at concentrations of 0% (square), 20% (triangle), or 40% (circle). Whole blood was then stimulated with or without various concentrations of ADP, as described in the Materials and Methods section. Values are the means ± SE of 4 experiments. $^{*}p < 0.05$, $^{**}p < 0.01$, compared with control (0% HbV).

agonist, was examined. Without ADP stimulation, a slight, but significant, reduction in the spontaneous release of TXB_2 from platelets pretreated with 40% HbV was observed (Fig. 2A). Similarly, the levels of spontaneous release of RANTES from platelets pretreated with both 20% and 40% HbV were slightly, but significantly, reduced in comparison with those from platelets that were not pretreated with HbV (0% HbV). The treatment of PRP with ADP caused a significant increase in the levels of each mediator in the releasates. Pretreatment of PRP with either 20% or 40% HbV did not affect the ADP-induced release of each mediator, although a slight reduction was observed in each case (Fig. 2).

Effect of HbV on Secretion of Platelet-derived Mediators in Resting and Collagen-stimulated Platelets In Vitro

The effect of HbV on mediator release was further examined using platelets stimulated with or without collagen, a strong platelet agonist. Without collagen stimulation, the levels of serotonin, TXB_2, and β-TG were not affected in the cell-free releasates from PRP after pretreatment with either 20% or 40% HbV, although the RANTES levels were slightly, but significantly, reduced ($p < 0.05$) (Fig. 3). Collagen stimulation of the PRP caused a marked increase in the levels of each mediator but pretreatment with 20% or 40% HbV did not affect the collagen-induced release of TXB_2, RANTES, or β-TG. The levels of serotonin in the collagen-stimulated PRP tended to decrease in an HbV-dose dependent manner.

DISCUSSION

In this study, the effect of HbV on the expression of platelet activation markers in the presence or absence of platelet agonists was evaluated in vitro. Integrin $\alpha_{IIb}\beta_3$ mediates platelet adhesion and aggregation and plays a crucial role in thrombosis and hemostasis [18]. $\alpha_{IIb}\beta_3$ is expressed in a low affinity state on resting platelets. On platelet activation, $\alpha_{IIb}\beta_3$ shifts to a high affinity conformation that efficiently binds its ligands, including fibrinogen and von Willebrand factor. Thus, such activation is a prerequisite for fibrinogen binding to platelets, which culminates in platelet aggregation. The high affinity conformation of $\alpha_{IIb}\beta_3$ on human platelets can be detected by the monoclonal antibody PAC-1 [15, 16, 19]. Because low doses of ADP cause an increase in PAC-1 binding within a short time period, this phenomenon is regarded as one of the earliest events in platelet activation, and PAC-1 has been shown to be a highly sensitive and specific marker of platelet activation [15, 16].

Activated platelets secrete a number of prothrombotic substances, like TXA_2, serotonin, and CD62P that act synergistically to form thrombi. TXA_2 is synthesized via the cyclooxygenase-mediated arachidonic

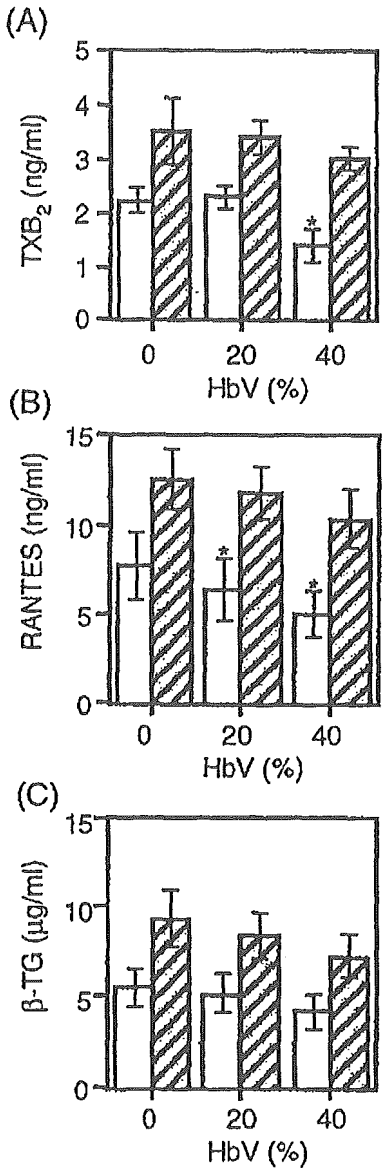

Figure 2. Effect of HbV on ADP-induced platelet mediator release. ADP-induced release of (A) TXB_2, (B) RANTES, and (C) β-TG from human platelets. PRP was incubated with concentrations of 0%, 20%, or 40% HbV and then stimulated with (hatched columns) or without (open columns) ADP, as described in the Materials and Methods section. Values are the means ± SE of 5 (A) and 6 (B, C) experiments using blood from different donors. *$p < 0.05$, compared with control (0% HbV).

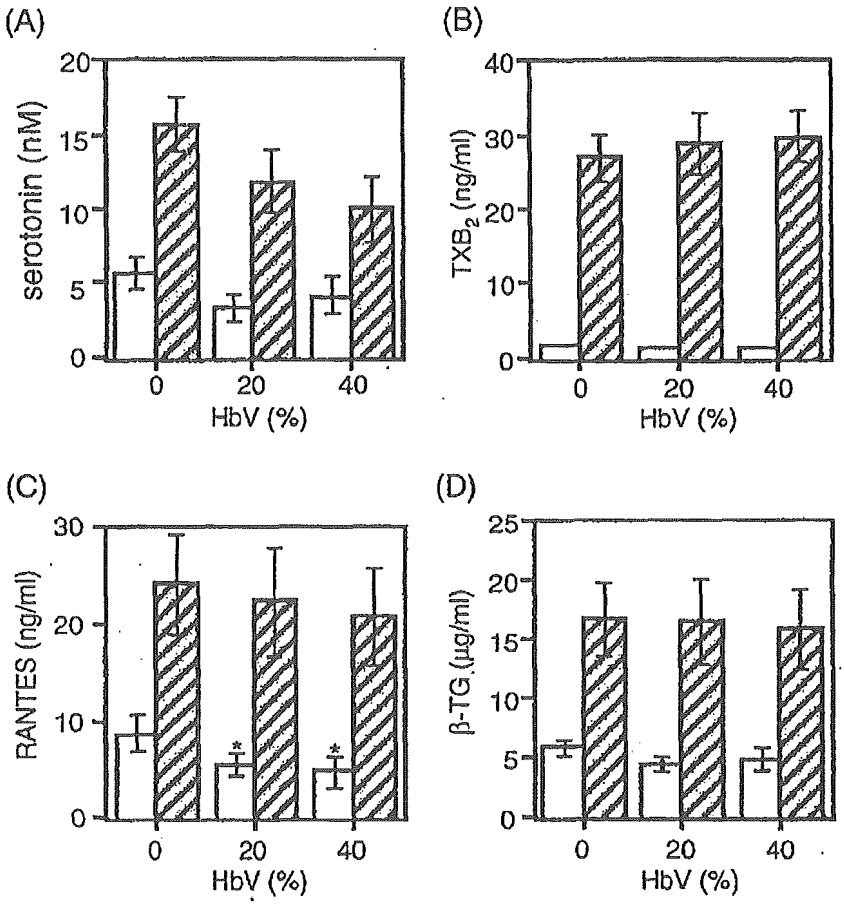

Figure 3. Effect of HbV on collagen-induced platelet mediator release. Collagen-induced release of (A) serotonin, (B) TXB_2, (C) RANTES, and (D) β-TG from platelets. PRP was incubated with concentrations of 0%, 20%, or 40% HbV and then stimulated with (hatched columns) or without (open columns) collagen, as described in the Materials and Methods section. Values are the means ± SE of 5 experiments using blood from different donors. *$p < 0.05$, compared with control (0% HbV).

metabolic pathway [20] and is a potent platelet agonist that induces a rapid positive feedback loop, thereby amplifying the activation signals and enabling robust platelet recruitment at the site of vascular injury [21]. Serotonin is a bioactive amine that localizes in dense granules of resting platelets and is secreted upon platelet activation. Serotonin also has a prothrombotic effect on platelets [12]. Interactions between platelets via CD62P stabilize the initial $\alpha_{IIb}\beta_3$–fibrinogen interactions, thereby promoting the formation of large, stable platelet aggregates

[22]. In addition, CD62P is the major surface receptor for neutrophils and monocytes on activated platelets, mediating leukocyte adhesion. Thus, platelet CD62P is involved in the recruitment of both platelets and leukocytes into an evolving thrombus [22–25].

Recent studies have extended platelet function to include the modulation of local inflammatory events through the release of chemokines and cytokines [13]. RANTES and β-TG [13] are stored in α-granules in platelets and are released from platelets on activation. RANTES has diverse inflammatory effects, such as histamine release from basophils and the exocytosis of eosinophil cationic protein. Furthermore, RANTES is a powerful chemoattractant for T cells, basophils, and eosinophils [13, 26]. β-TG, a platelet-derived CXC chemokine, is also released into the blood at micromolar concentrations and plays an important role in the recruitment of neutrophils to sites of tissue injury [27]. Consequently, the aberrant release of serotonin, TXA_2, RANTES, or β-TG in response to the inappropriate activation of platelets could result in pathological thrombosis, inflammatory reactions, or allergic responses.

The present study demonstrated that the exposure of blood samples to HbV at concentrations of up to 40% did not cause platelet activation, as measured by various markers, although the levels of RANTES and TXB_2 were significantly, but marginally, reduced. In terms of the effect of HbV on platelet activation triggered by submaximal concentrations of agonists, the enhancement of PAC-1 binding to platelets, one of the earliest markers of activation, was observed after the exposure of blood samples to HbV at concentrations of up to 40%, suggesting that HbV might have an enhancing effect on agonist-induced platelet aggregation. Other than the slight enhancing effect of HbV on PAC-1 binding in the presence of agonist stimulation, however, none of the other parameters were significantly affected. Rather, the levels of TXB_2, RANTES, and β-TG tended to be reduced by ADP stimulation, while the level of serotonin tended to be reduced by collagen stimulation. Thus, the lack of coordinated potentiation in the levels of prothrombotic substances (i.e., TXB_2 and serotonin) and stabilizing molecules involved in the initial $\alpha_{IIb}\beta_3$–fibrinogen interactions (i.e., CD62P) in response to the presence of an agonist suggests that the enhancing effect of HbV on platelet reactivity to agonists, if present, is not likely to lead to the deleterious formation of thrombi. In addition, the absence of adverse effects on the secretion of RANTES and β-TG suggest that HbV is unlikely to trigger the initiation and/or aberrant perpetuation of inflammatory and allergic reactions.

The present results are of value for estimating the biocompatibility of HbV and human platelets. Further research is warranted to investigate whether the administration of HbV has any effect on platelet activation and platelet functions in vivo.